The Structure of Metallomicelles

P. C. Griffiths,*[a] I. A. Fallis,*[a] D. J. Willock,[a] A. Paul,[a] C. L. Barrie,[a] P. M. Griffiths,[a] G. M. Williams,[a] S. M. King,[b] R. K. Heenan,[b] and Richard Görgl[c]

Abstract: The morphology of micelles formed by two novel metallosurfactants has been studied by small-angle neutron scattering (SANS) and small-angle-X-ray scattering (SAXS). The two surfactants both contain a dodecyl chain as the hydrophobic moiety, but differ in the structure of the head group. The surfactants are Cu^{II} complexes of monopendant alcohol derivatives of a) the face-capping macrocycle 1,4,7-triazacyclanonane (tacn), and b) an analogue based upon the tetraazamacrocycle 1,4,7,10-tetraazacyclododecane. Here, neutron scattering has been used to study the overall size and shape of the surfactant micelles, in conjunction with X-ray scattering to locate the metal ions. For the 1,4,7,10-tetraazacyclododecane-based surfactant, oblate micelles are observed, which are smaller to the prolate micelles formed by the 1,4,7-triazacyclononane analogue. The X-ray scattering analysis shows that the metal ions are distributed throughout the polar head-group region, rather than at a well-defined radius; this is in good agreement with the SANS-derived dimensions of the micelle. Indeed, the same model for micelle morphology can be used to fit both the SANS and SAXS data.

Keywords: aggregation · macrocyclic ligands · SANS · SAXS · surfactants

Introduction

The incorporation of transition metal centers into surfactant molecules provides a means of localizing many of the physicochemical properties of these ions at oil–water or water–air interfaces. Although such surfactants are comparatively rare,[1] they have recently found important potential applications in diverse subject areas such as magnetic resonance imaging,[2] the templating of mesoporous materials,[3] vesicle formation,[4] laser-induced fluorescence,[5] thin-film optoelectronics,[6] interfacial photophysics,[7] homogeneous catalysis[8] and as anthelmintic therapeutics[9]. The SANS and SAXS study is presented in this paper and is part of a program to investigate structure-property relationships in such systems.[10] Here, we have set out to examine the role that the head group structure plays in determining micellar morphology and we have used a combination of neutron and X-ray scattering in order to generate a more detailed picture of micellar morphology. It is interesting to note that whilst there is a large body of literature describing SANS[11] or SAXS[12] studies on micellar systems, relatively few groups have applied both techniques[13] to a common system.

Metallosurfactants are ideally suited to be studied by using a combination of SANS and SAXS. Neutron scattering of proteo-surfactants in deuterated media allows the character of the micelle core and polar shell regions to be analysed within the context of a particular model, whilst X-ray scattering from the heavy atom (metal cation), which contains head group, permits a complimentary picture of the interfacial region to be determined. The study described by Arleth and co-workers[14] is the only combined SAXS/SANS examination of a metallosurfactant previously reported to date.

In designing a metal containing surfactant system it is important that the metal cation be bound very strongly to the head group. This not only simplifies the system by reducing the number of components, but also prevents the erroneous determination of CMC (critical micelle concentration) values, which is caused by the presence of surface-active or water-immiscible ligands. Thus, we have devised a simple synthesis of water-insoluble ligands based upon the reaction of macrocyclic polyamines agents and terminal epoxides.[10] This approach allows both the length of the hydrophobe and, by choice of different macroyclic donors, the size and structure of the head group to be varied easily. The effect of surfactant head-group structure on the micelle morphology

[a] Dr. P. C. Griffiths, Dr. I. A. Fallis, Dr. D. J. Willock, Dr. A. Paul, C. L. Barrie, Dr. P. M. Griffiths, Dr. G. M. Williams
Department of Chemistry, Cardiff University
PO Box 912, Cardiff CF10 3TB (UK)

[b] Dr. S. M. King, Dr. R. K. Heenan
ISIS Facility, Rutherford Appleton Laboratory
Chilton, Didcot OX11 0QX (UK)

[c] Dr. R. Görgl
Materials Center Leoben & Erich-Schmid-Institute
Berlin (Germany)

DOI: 10.1002/chem.200305670

is reported here for two Cu^{II}, which contain surfactants based upon the ligands 1-(2-hydroxytetradecyl)-1,4,7-triazacyclononane (**1**) and 1-(2-hydroxytetradecyl)-1,4,7,10-tetraazacyclododecane (**2**) (Scheme 1).

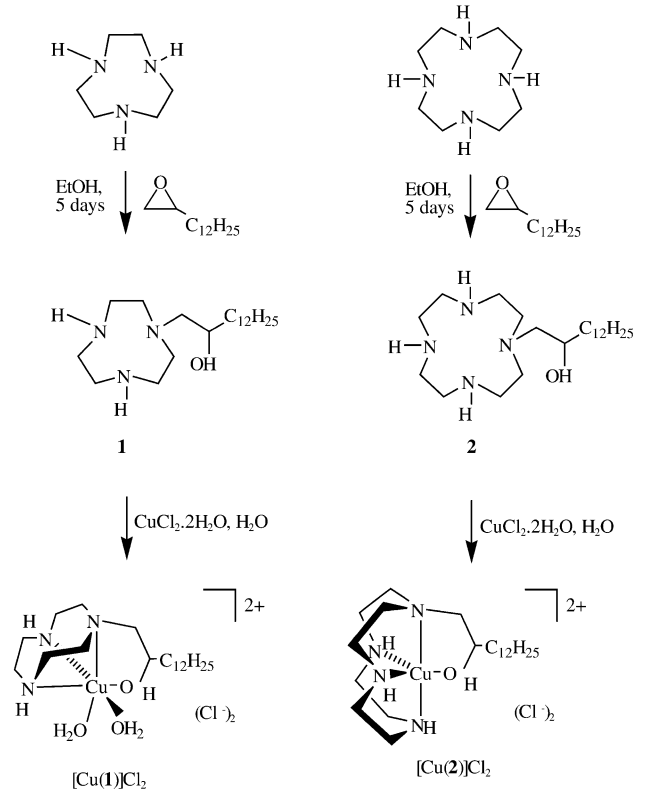

Scheme 1. Ligand syntheses and proposed structures of the a) [Cu^{II}(**1**)-$(H_2O)_2$]Cl_2 and b) [Cu^{II}(**2**)]Cl_2 cationic surfactants.

Experimental Section

Surfactant synthesis: 1,4,7-Triazacyclonane was prepared by using standard methods,[15] and was purified (twice) by bulb-to-bulb distillation prior to use. 1,4,7,10-Tetraazacyclododcene was purchased from Strem and sublimed prior to use. All other reagents (Aldrich, Avocado) were used as received. Solvents were purified by standard literature methods.[16] Electronic spectra were recorded in acetonitrile solution by using Jasco V-570 NIR-UV-vis spectrometer. NMR spectra were obtained on Brüker AMX 400 or Jeol Eclipse 300 spectrometers, and referenced to external TMS.

1,2-Tetradecanediol: Potassium ferricyanide (29.6 g, 90 mmol), potassium carbonate (12.45 g, 90 mmol), 1-tetradecene (5.95 g, 30 mmol) potassium osmate (45 mg, 0.4 mol%), and quinuclidine (33 mg, 1 mol%) was added to a flask containing *tert*-butanol/water (300 ml, 50:50). After stirring for 72 h, sodium sulfite (135 g, 1.07 mol) was added, and the solution stirred for a further two hours. Water (75 ml) was added and the aqueous phase extracted with dichloromethane. The combined organic extracts were washed with water and dried over magnesium sulfate. The solvent was stripped by rotary evaporation to yield a crude product which was recrystallised from ethyl acetate to yield a white solid, 6.15 g (88%) m.p. 64–66 °C; ^{1}H NMR (400 MHz, $CDCl_3$) $\delta = 0.88$ (t, $J = 7$ Hz, 3H; -CH_3), 1.26 (m, 20H; -CH_2-), 1.62 (m, 2H; -HOCHCH_2CH$_2$-), 1.93 (m, 1H; HOCH$_2$-), 2.05 (m, 1H; CHOH), 3.44 (m, 1H; CH_2OH), 3.68 ppm (m, 2H; -CHOHCH_2OH); ^{13}C NMR ($CDCl_3$) $\delta = 72.3$, 66.84, 33.18, 31.91, 29.63, 29.58, 29.54, 29.35, 25.52, 22.69, 14.13 ppm; IR (KBr disc): $\tilde{\nu} = 3200.4$, 2916.6, 2847.9, 1466.2, 1074.7 cm^{-1}; mass spectrum (EI): m/z (%) 213 (20), 199(78), 124(65), 110(76), 60(100); elemental analysis calcd (%) for $C_{14}H_{30}O_2$: C 72.99, H 13.12; found: C 72.87, H 13.23.

1,2-Epoxytetradecane: 1,2-Tetradecanediol (5 g, 24 mmol) was added to a solution of HBr/acetic acid (45% w/v) (20 ml) and the resulting solution was stirred vigorously for 30 mins. The reaction mixture was diluted with water and extracted with dichloromethane. The combined organic extracts were washed with water and dried over magnesium sulfate. Evaporation of the solvent afforded a crude oil. Dry methanol (20 ml) and potassium carbonate (4.98 g, 36 mmol) were added and the reaction was stirred for a further 2 h. The reaction was quenched with water and extracted with dichloromethane. The combined organic extracts were washed with water and dried over magnesium sulfate. Filtration through a short silica column and evaporation of the solvent afforded an oil, which was distilled (twice) by using a Kügelrohr apparatus to yield a clear oil 4.3 g (93%); ^{1}H NMR (400 MHz, $CDCl_3$) $\delta = 0.88$ (t, $J = 7$ Hz, 3H; -CH_3), 1.26 (m, 18H; -(CH_2)$_9$CH$_3$), 1.45 (m, 2H; -CHCH$_2$CH_2-), 1.53 (m, 2H; CHCH_2-), 2.47 (dd, $J = 5$, 3 Hz, 1H; OCH_2CH-), 2.75 (t, $J = 5$ Hz, 1H; OCH_2CH-), 2.91 ppm (m, 1H; OCH$_2$CH-); ^{13}C NMR ($CDCl_3$) $\delta = 52.42$, 47.15, 32.49, 31.90, 29.66, 29.63, 29.55, 29.44, 29.35, 25.97, 22.69, 14.12 ppm; IR (KBr disc): $\tilde{\nu} = 3040.8$, 2926.3, 2854.7, 1466.0, 1258.4, 1129.6, 914.9, 836.1, 721.6 cm^{-1}; mass spectrum (APCI); m/z (%) 213 [M^++1] (100); elemental analysis calcd (%) for $C_{14}H_{28}O$: C 79.18, H 13.29; found: C 79.20, H 13.26.

1-(2-Hydroxytetradecyl)-1,4,7-triazacyclononane (1): 1, 2-Epoxytetradecane (849 mg, 4 mmol) was added to a flask containing freshly distilled 1,4,7-triazacyclononane (5.16 g, 40 mmol) in degassed ethanol (30 ml). The solution was left to stand for seven days. Evaporation of the solvent afforded a crude oil which was subjected to bulb-to-bulb distillation (Kugelröhr, 0.005 mmHg) to remove excess 1,4,7-triazacyclononane (140 °C). The oven temperature was raised to 200 °C to yield the required product as a clear colourless oil (1.36 g, quantitative); ^{1}H NMR (400 MHz, $CDCl_3$) $\delta = 0.87$ (t, $J = 7$ Hz, 3H; -CH_3), 1.24 (m, 20H; -(CH_2)$_{10}$CH$_3$), 1.48 (m, 1H; -CHOHCH_2CH$_2$-), 2.32 (dd, $J = 13$, 11 Hz, 1H; -CHOHCH_2CH$_2$-), 2.62–2.80 (m, 14H; -NCH_2-), 3.09 (br s, 2H; -NH), 3.62 ppm (m, 1H; -CHOH-); ^{13}C NMR ($CDCl_3$) $\delta = 14.11$, 22.67, 25.95, 29.34, 29.59, 29.62, 29.65, 29.85, 31.9, 34.61, 46.53, 47.24, 52.99, 63.27, 69.15 ppm; IR (KBr disc): $\tilde{\nu} = 3320.6$, 2919.7, 2855.3, 1667.1, 1459.5, 1352.1, 1294.8, 1115.9, 1072.9, 979.9, 722.2 cm^{-1}; mass spectrum (EI), m/z (%) 341 [M^+] (20), 297 (40), 285 (70), 256 (100).

1-(2-Hydroxytetradecyl)-1,4,7,10-tetraazacyclononane (2): This material was prepared in an analogous manner to that for **1** by using freshly sublimed 1,4,7,10-tetraazacyclononane (6.89 g, 40 mmol) and 1,2-epoxytetradecane (849 mg, 4 mmol). Bulb-to-bulb distillation at 220 °C afforded the title compound as a waxy white solid (1.53 g, quantitative); ^{1}H NMR (400 MHz, $CDCl_3$) $\delta = 0.87$ (t, $J = 7$ Hz, 3H; -CH_3), 1.24 (m, 22H; -(CH_2)$_{11}$CH$_3$), 2.35–2.81 (m, 18H; -NCH_2-), 3.68 ppm (m, 1H; -CHOH-); ^{13}C NMR ($CDCl_3$) $\delta = 14.11$, 22.68, 25.79, 29.34, 29.61, 29.63, 29.66, 29.82, 31.90, 34.67, 46.00, 46.89, 47.56, 52.86, 61.89, 68.91; IR (KBr disc): $\tilde{\nu} =$ 3286.3, 2922.7, 2852.1, 1656.7, 1464, 1352, 1275, 1114, 1041, 953, 754 cm^{-1}; mass spectrum (APCI): m/z (%) 385 [M+1] (100).

Complex formation: Cu^{II} complexes of (**1**) and (**2**) were prepared by the addition of 1.05 equivalents of $CuCl_2$·2H_2O to a suspension of the ligand in D_2O in volumetric flasks. The reaction mixtures were gently warmed to effect complete dissolution of the ligands and diluted to the appropriate concentration with D_2O. The electronic spectra of these complexes were measured as a means of determining their structures in solution (see Results and Discussion).

Small-angle neutron scattering (SANS): Small-angle neutron scattering (SANS) measurements were performed on the fixed-geometry, time-of-flight LOQ diffractometer (ISIS Spallation Neutron Source, Oxfordshire UK). By using neutron wavelengths spanning 2 to 10 Å, a Q-range of approximately 0.015 to 0.20 Å^{-1} (50 Hz) was accessible, with a sample-detector distance of 4.1 m.

The surfactant solutions at surfactant concentration of 25 mM and 50 mM were dissolved in D_2O, placed in 2 mm pathlength quartz cuvettes (Hellma) and mounted in aluminium holders on top of an enclosed, computer-controlled, sample changer. Temperature stability of ±0.2 °C was achieved by the use of a thermostated circulating bath-pumping fluid through the base of the sample changer. All measurements were carried

out at 45 °C, since the surfactant has a Krafft point around room temperature. Experimental measuring times were between 80 and 120 minutes.

All scattering data were a) normalised for the sample transmission and incident wavelength distribution, b) background corrected by using an empty quartz cell, which also removes the inherent instrumental background arising from vacuum windows, and so on and c) corrected for the linearity and efficiency of the detector response. The data were put onto an absolute scale by reference to the scattering from a well-characterised partially-deuterated polystyrene-blend standard sample.

Small-angle X-ray scattering (SAXS): The SAXS measurements were performed on a HR-PNK pinhole camera at the NanoSTAR facility, housed within the Materials Center of the Leoben & Erich-Schmid-Institute. A ceramic X-ray tube provided a 2.2 kW beam 0.4 mm by 12 mm in size. The K_α of copper was used to generate a 40 kV beam of the same dimension. Pinhole dimensions of 750 μm (first), 400 μm (second) and 1000 μm (third) were used and the instrument configured based on the following distances; source to 1st pinhole: 200 mm; 1st pinhole to 2nd: 925 mm; 2nd pinhole to 3rd: 482 mm; 3rd pinhole to sample: 35 mm; the sample to detector distance was 640 mm. A similar configuration has been described by Pedersen.[17] A Bruker AXS HI-STAR position sensitive area detector recorded the intensity of the scattered X-rays as a function of angle and thus, wavevector.

Samples were contained within capillaries of quartz glass, which were 2 mm in diameter. The measuring time was 20000 s. Sample transmissions have been calculated by using the "indirect" method through a strongly scattering standard (glassy carbon) and a background of distilled water subtracted from the data.

Results and Discussion

Synthesis of materials: The syntheses of the ligands **1** and **2** were carried out in straightforward manner as shown in Scheme 1. It was found that is was necessary to prepare fresh 1,2-epoxytetradecane from the corresponding diol, since commercial sources of long chain racemic diols are contaminated with varying amounts of isomeric branched materials; these are difficult to remove by chromatography or distillation. 1,2-Tetradecanediol is a crystalline solid that may be purified by repeated crystallisation from ethyl acetate with subsequent conversion to the terminal epoxide yielding the required precursor free of any branched material. Reaction with an excess of 1,4,7-triazacyclononane or 1,4,7,10-tetraazacyclododecane upon removal of excess macrocycle affords **1** and **2** in quantitative yield. The recovered macrocycle may be recycled and used in subsequent syntheses. This synthesis, whilst requiring large quantities of purified macrocyclic precursors, was found to yield purer materials than when the previously described protective group methodologies were employed.[18] The free ligands **1** and **2** are essentially insoluble in water, but dissolve rapidly upon the addition of $CuCl_2{\cdot}2H_2O$ to afford blue (**1**) or purple (**2**) solutions formulated as $[Cu^{II}(\mathbf{1})(H_2O)_2]Cl_2$ (aq.) and $[Cu^{II}(\mathbf{2})]Cl_2$ (aq.), respectively. We can be confident of an approximate octahedral geometry at the metal centre in the case of $[Cu^{II}(\mathbf{1})(H_2O)_2]Cl_2$ from the presence of a single unsymmetrical d–d band ($\lambda = 664$ nm, $\varepsilon = 52\ L\,mol^{-1}\,cm^{-1}$) in the electronic spectrum.[19] In the case of $[Cu^{II}(\mathbf{2})]Cl_2$ we assign a five coordinate structure from the electronic spectrum, which consists of a single broad intense peak ($\lambda =$ 568 nm, $\varepsilon = 199\ L\,mol^{-1}\,cm^{-1}$); this is typical of a five coordinate Cu^{II} species with mixed nitrogen/oxygen ligand-donor atom arrays.[19] The proposed structures of the surfactants are shown in Scheme 1. Given the very high formation constants typical of macrocyclic amine ligands[20] and the rapid kinetics of Cu^{II} complex formation, we can be confident that there was essentially no free ligand in the presence of a slight excess of metal cation.

Scattering analysis: Arleth et al.[14] in their SANS-SAXS study of 1,8-bis[*N*-β-D-glucopyranosyl-*N*-octyl-2-(carboxamidoethyl)]-1,4,8,11-tetraazacyclotetradecane with complexed Cu^{II} cations (as the fluoride salt) adopted two approaches to extract the morphology of the aggregates from their scattering data. The first was a model independent approach centred on a indirect Fourier transform of the scattering data and subsequent square-root deconvolution of the pair-distance distribution to yield the scattering-length density profile across the aggregate. The second was model dependent and assumes (based on the model-free approach) that the micelles are monodisperse and can be described as short core-shell rods with no solvent penetration into the micellar core. In the present study, we have also adopted a model dependent approach. Various models were tested (sphere, ellipse, rod etc.,) in which it was necessary to limit or constrain some of the parameters to known or calculated values. In particular, the volumes and scattering length densities of the constituent moieties within the surfactant. Such an approach to fitting SANS scattering has been described in detail elsewhere[21] and only the essential details are reported here.

The model of the micelle adopted here is that of a charged particle with an elliptical core-shell morphology and therefore, the intensity of scattered radiation, $I(Q)$, as a function of the wave-vector, Q, is given by Equation (1) below,

$$I(Q) = n_m\left[S(Q)\langle F(Q)\rangle^2 + \langle |F(Q)|^2\rangle - \langle F(Q)\rangle^2\right] + B_{inc} \qquad (1)$$

in which $F(Q) = V_1(\rho_1 - \rho_2 F_0(QR_1) + V_2(\rho_2 - \rho_{solvent})F_0(QR_2)$. For an elliptical micelle, both $F(Q)$ and $F(Q)^2$ require numerical integration over an angle γ between Q and the axis of the ellipsoid to account for the random distribution of orientations of the ellipse. For clarity, we have omitted this. The first term in [Eq. (1)] represents the scattering from the core (subscript 1) and the second, the polar shell (subscript 2). $V_i = \frac{4}{3}\pi R_i^3$ and $F_0(QR_i) = \frac{3j_i(QRi)}{QRi}$ (j_i is the first-order spherical Bessel function of the first kind). $S(Q)$ represents the spatial arrangement of the micelles in solution and n represents the micelle number density.

ρ is the neutron scattering length density of the micellar core (subscript 1), the polar shell (subscript 2) and the solvent (subscript 0). These constants are combined into a single fit parameter used to "scale" the model intensity to the absolute value. Post-fitting, this scalar is recalculated by using the parameters describing the micelle morphology/composition and the molar concentration of micelles to validate the fit. The calculated and observed values should lie within ~10%.

It is expedient here to limit the number of adjustable parameters within the core-shell fit and this is most conven-

iently undertaken by constraining the minor radius of the ellipse representing the hydrophobic core to be 16.7 Å (the all-*trans* length of a dodecyl tail) and thus, its scattering length density to be that of dodecane. The remaining "fragments" are somewhat arbitrarily assigned to the head group region.

Based on this delineation of tail and head group regions, the model can be further refined by calculating the volume and scattering length density of the anhydrous surfactant head groups. As an estimate, we have computed the surface area of the head group by using a DFT routine ADF 2.3[22] based on a triple zeta basis set and polarization functions on all atoms except the metal. From this surface area, an effective spherical volume is calculated having incorporated 30 $Å^3$ for the OH group, 27 $Å^3$ for each of the two -CH_2- groups and 73 $Å^3$ for the metal and chloride ions.

Modelling of the structure of the head group region is complicated, because the chloride counterions have the potential, to some degree, to dissociate from the micelle. This parameter is not known, so we have predicted that 75% of the chlorides are electrostatically bound to the micelle surface. The maximum error in both the head group scattering length density and head group volume introduced by using this assumption is less than 10%; this is well within experimental error for example, for $[Cu^{II}(\mathbf{2})]Cl_2$, (i.e., no dissociation) $\rho_{\text{head group}} = 0.90 \times 10^{-6}$ $Å^{-2}$, $V_{\text{head goup}} = 475$ $Å^3$; $[Cu^{II}(\mathbf{2})]^{2+}$ Cl^- (i.e. 50% dissociation); $\rho_{\text{head group}} = 0.75 \times 10^{-6}$ $Å^{-2}$, $V_{\text{head goup}} = 450$ $Å^3$. We have adopted a 25% degree of dissociation and thus, the volume of the polar head is 465 $Å^3$ for $[Cu^{II}(\mathbf{2})]Cl_2$ and 420 $Å^3$ for $[Cu^{II}(\mathbf{1})(H_2O)_2]Cl_2$. The corresponding scattering length densities of the anhydrous headgroups are very similar, 0.83×10^{-6} $Å^{-2}$ and 0.81×10^{-6} $Å^{-2}$ for $[Cu^{II}(\mathbf{2})]Cl_2$ and $[Cu^{II}(\mathbf{1})(H_2O)_2]Cl_2$, respectively.

The structure factor $S(Q)$ was calculated by using the Hayter and Penfold model[23] for spheres of a given micellar charge and ionic strength, which incorporates refinements for low volume fractions and a penetrating ionic background. This $S(Q)$ also requires the hard-sphere radius, the total volume fraction of the hard spheres and the inverse Debye length. The hard-sphere radius was allowed to vary but the volume fraction was constrained to a value calculated from the mass concentration and density. This method of calculating the structure factor, which assumes spherical particles, remains valid for randomly orientated micelles with small degrees of ellipticity, as is the case here. The ionic strength is governed by the concentrations of the unimeric surfactant, the free chloride counter-ions of the micelle surfactant and any added salt. The last contribution is again calculated based on the assumption of 25% dissociation of the chloride counterions.

In summary, the minor radius, the ratio of head group to tail volumes, the scattering length densities of the anhydrous head group and core regions, the volume fraction and ionic strength are inputted as constants. The only fitting parameters describing the form factor $P(Q)$ are the ellipticity X of the micelle and the volume fraction of water in the head group region. The thickness and scattering length density of the hydrated head group region are (re-)calculated within the analysis software and are based on the fraction of water in the shell, ϕ_{water}. The only fitting parameters in the structure-factor calculation are the charge and the hard-sphere radius.

The scattering from 50 mM $[Cu^{II}(\mathbf{2})]Cl_2$ (aq.), 25 mm $[Cu^{II}(\mathbf{1})(H_2O)_2]Cl_2$ (aq.) and 50 mM $[Cu^{II}(\mathbf{1})(H_2O)_2]Cl_2$ (aq.), all in the presence of a slight excess amount of $CuCl_2$, are shown in Figure 1, 2 and 3, respectively as a function of

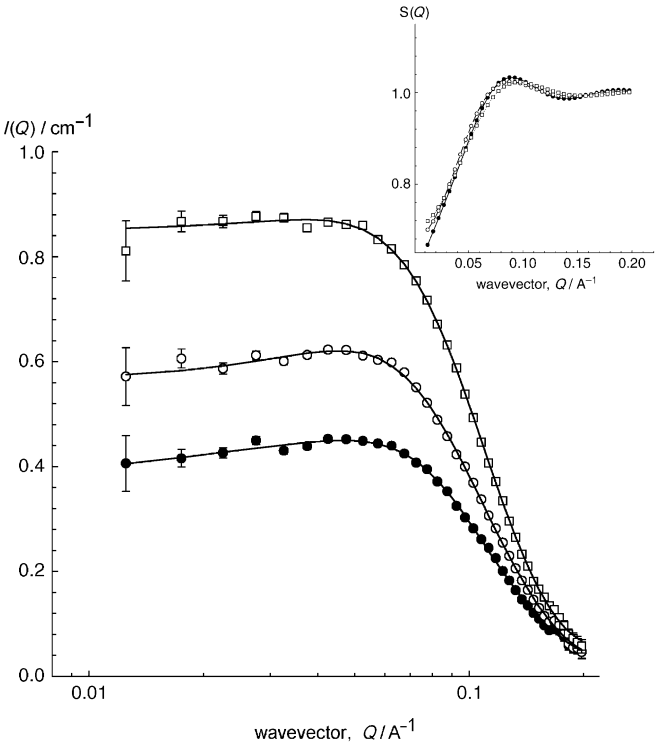

Figure 1. SANS from 50 mM solutions of $[Cu^{II}(\mathbf{2})]Cl_2$ in D_2O as a function of added electrolyte (NaCl); (●) 0 mM; (○) 40 mM and (□) 100 mM. Solid lines correspond to the fit to the core-shell model by using the parameters given in Table 1; inset: Hayter-Penfold $S(Q)$ derived from analysis of the SANS given in Figure 1 (●) 0 mM; (○) 40 mM and (□) 100 mM.

ionic strength. The scattering curves for **1** and **2** systems are very different, which suggests that the micelle morphology is not the same for the two cases. Pertinent parameters describing the fits to the core-shell model are presented in Table 1.

Consider first the $[Cu^{II}(\mathbf{1})(H_2O)_2]Cl_2$ (aq.) system, Figure 1. With increasing ionic strength, the scattering curves are displaced vertically, but essentially are very similar in shape. By simple inspection, we might expect to find that the smaller dimension associated with the micelle morphology is increasing based on the increase in slope at higher Q (higher Q corresponds to smaller dimensions or distance scales), but that the larger dimension is largely unchanged (the similar shape at low Q). The scattering behaviour at low Q is also modulated by any changes in the structure factor, which may also contribute to the vertical offset in intensity.

From the fitted data, it may be seen that there is very little change in the structure factor, Figure 1 inset, and it is therefore the form factor, the size and shape of the micelle, that accounts for the differences in the scattering behaviour.

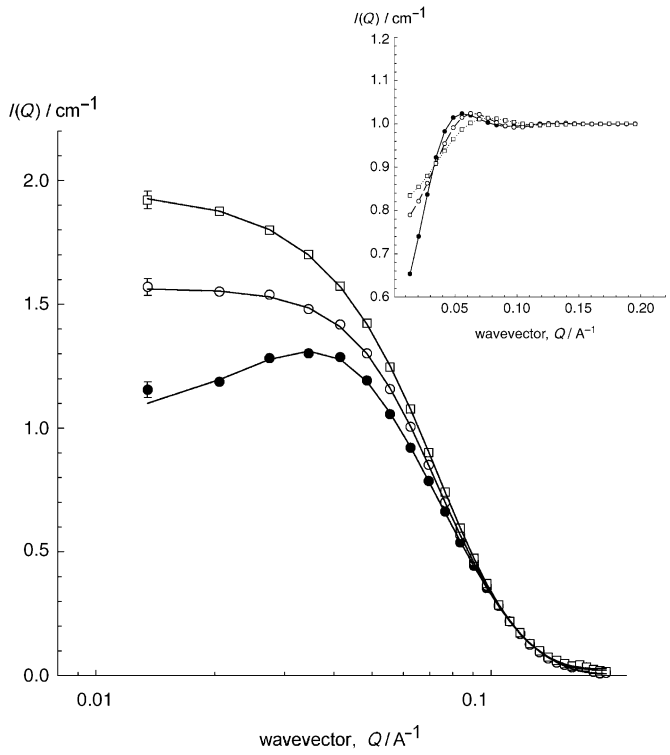

Figure 2. SANS from 25 mM solutions of $[Cu^{II}(\mathbf{2})(H_2O)_2]Cl_2$ in D_2O as a function of added electrolyte (NaCl); (●) 0 mM; (○) 40 mM and (□) 100 mM. Solid lines correspond to the fit to the core-shell model by using the parameters given in Table 1; inset: Hayter-Penfold $S(Q)$ derived from analysis of the SANS given in Figure 2; (●) 0 mM; (○) 40 mM and (□) 100 mM.

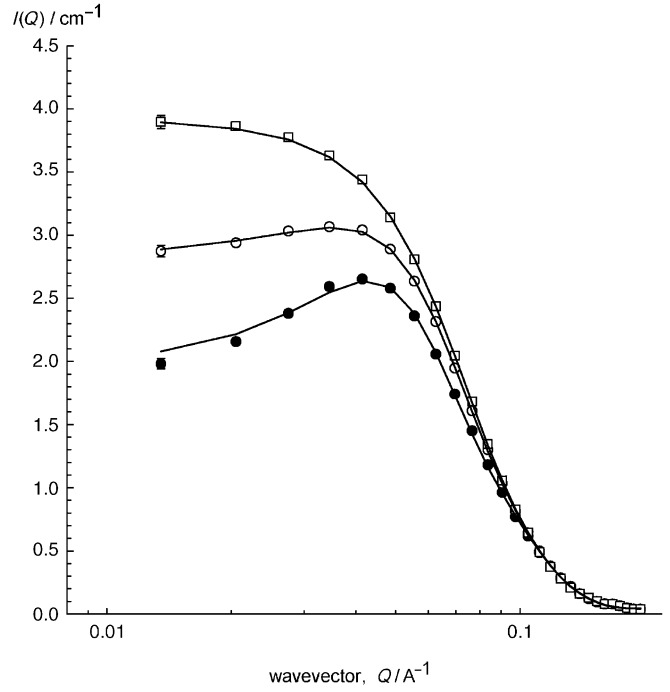

Figure 3. SANS from 50 mM solutions of $[Cu^{II}(\mathbf{1})(H_2O)_2]Cl_2$ in D_2O as a function of added electrolyte (NaCl); (●) 0 mM; (○) 40 mM and (□) 100 mM. Solid lines correspond to the fit to the core-shell model by using the parameters given in Table 1.

As shown in Table 1, as the degree of ellipticity increases, the micelles become less disc-like (oblate), since the ionic strength increases. Concomitantly, the aggregation number increases. The effective scattering length density of the shell is significantly greater than the calculated scattering length density of the "dry" head groups ($\rho_{shell} \approx 0.87 \times 10^{-6}$ Å^{-2}), which indicates that the head groups are well solvated and become more so with increasing ionic strength. It is tacitly assumed in these calculations that the majority (~75%) of the chloride counterions are bound to the micelle surface, which suggests that the surfactant has rather a more nonionic character than cationic, an assumption supported by the insensitivity of the $S(Q)$ to added electrolyte. The scattering from the **1** (25 mM) solutions are also very similar (not shown), but they have a greater signal to noise due to the decrease in surfactant concentration. Nonetheless for each ionic strength, the same parameters fit both the 25 mM and 50 mM data once the differing concentrations have been accounted for, thus lending considerable support to the choice of model.

The $[Cu^{II}(\mathbf{2})]Cl_2$ (aq.) system is quite different. The scattering curves change shape as the ionic strength is increased. The high Q behaviour is very similar for the three cases, which suggests that the smaller dimension describing the micelle shape does not change. The low Q behaviour is increasing in intensity coupled to a maximum which is becoming less pronounced as the ionic strength is increased. Hence, the large micelle dimension and/or the structure factor must be changing with ionic strength. As shown in Figure 2 inset, the data are strongly modulated by the structure factor, which in turn suggests that that the micelles have a greater ionic character compared to $[Cu^{II}(\mathbf{1})(H_2O)_2]Cl_2$.

The $[Cu^{II}(\mathbf{2})]Cl_2$ micelles are prolate ellipses, rod-like micelles (Table 1), with an ellipticity that increases with increasing ionic strength. The increasing micelle length, in conjunction with the $S(Q)$, accounts for the low Q behaviour. Concomitant with this shape change, is an increase in aggregation number. The effective scattering length density of the shell ρ_{shell} is comparable to the $[Cu^{II}(\mathbf{1})(H_2O)_2]Cl_2$, indicates that these head groups are also rather well solvated and these too become more hydrated with an increase in ionic strength. These seem like logical observations given the high hydrogen-bonding potential of the metal complex head-groups.

SAXS analysis: The micelle morphology is reflected in the location of the metal ion and can be probed by SAXS due to the very different X-ray scattering length of the copper ion compared to the largely hydrocarbon based ligand moieties. The two surfactants were indeed also examined by SAXS Figure 4 and 5 in the presence of the highest amount of salt to damp out the structure factor that would complicate the data analysis. Just as in the SANS data, the scattering observed is different again, which suggests that the micelle morphology is quite different in the two cases. Significantly, the initial decrease in the SAXS intensity is greatest for $[Cu^{II}(\mathbf{1})(H_2O)_2]Cl_2$, commensurate with a greater micelle size; this is in good agreement with the SANS analysis.

Table 1. Parameters describing the elliptical core-shell fit to the SANS data

	1 (25 mM) [NaCl]			**1** (50 mM) [NaCl]			**2** (50 mM) [NaCl]		
	0 mM	40 mM	100 mM	0 mM	40 mM	100 mM	0 mM	40 mM	100 mM
aggregation number (±5)	110		110		35				
shell thickness (±0.5) Å^{-1}	9.0		10.0		8.5				
ellipticity (± 0.1)	2.0			2.0			0.6		
charge (±1)	7	18	20	7	18	16	2	5	9
volume fraction of water in the head group region	0.5			0.5			0.6		
α_{Cl} (±0.05)	0.1	0.15	0.2	0.1	0.15	0.15	0.10	0.25	0.30

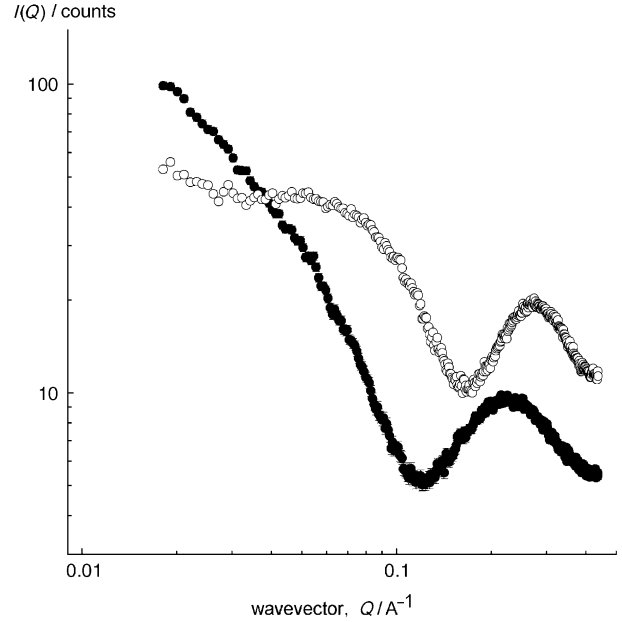

Figure 4. SAXS from 50 mM solutions of $[Cu^{II}(\mathbf{1})(H_2O)_2]Cl_2$ in 100 mM NaCl. Solid lines are best-fits to the data as described in the text. Also shown are fits with the metal distributed within a 4 Å shell (dotted line), 7 Å shell (dashed line), and 15 Å shell (dash-dot line).

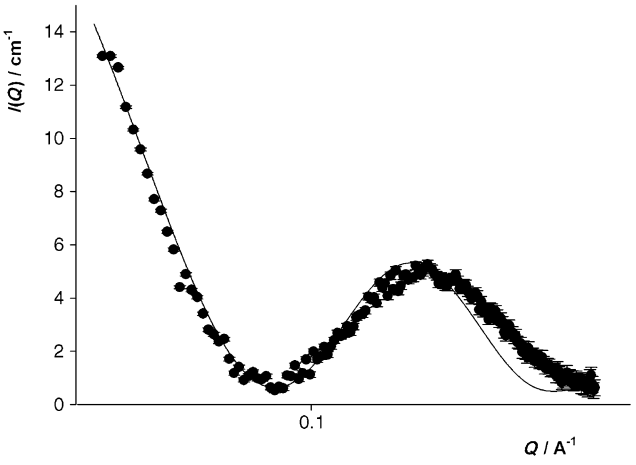

Figure 5. SAXS from 50 mM solutions of $[Cu^{II}(\mathbf{2})]Cl_2$ in 100 mM NaCl. The solid line is a best-fit to the data as described in the text.

It was hoped that since SAXS scattering increases with atomic number, the observed scattering would be dominated by the heavier metal ions. These are associated with the surfactant head group and thus, only the shell of the micelle would be observed. Initial attempts to fit the data focused on infinitely thin spherical shells as might be expected from a corona of metal ions. The principal variable was the radius of this corona.[14] Such approaches did not fit the data at all. Clearly, the metal ions are distributed throughout the diffuse head-group region rather than a thin shell.

Therefore, the SAXS data were fitted to the same core-shell ellipsoid model used to treat the SANS data. The model is analogous to that used to fit the neutron scattering data with the exception that X-ray scattering lengths are incorporated in place of neutron scattering lengths. Reassuringly, the overall size and shape of the micelles obtained were consistent with a prolate ellipse ($X=2$) for (**1**) and oblate ellipse ($X=0.6$) for (**2**).

Consider first the $[Cu^{II}(\mathbf{2})]Cl_2$ case, the data and fits are shown in Figure 4, which also demonstrates that in order to fit the data, a shell thickness of ~12 Å associated with a core radius of 16.7 Å was required. From space filling arguments, this equates to a volume fraction of water in the polar shell of ~0.7, that is, that the head groups are highly hydrated, a requirement consistent with that found from the more detailed core-shell analysis of the SANS data and as observed by Arleth et al. in their SANS-SAXS study of 1,8-bis[*N*-β-D-glucopyranosyl-*N*-octyl-2-(carboxamidoethyl)]-1,4,8,11-tetraazacyclotetradecane/copper fluoride complexes.[14] The equivalent quantity for the common surfactant sodium dodecylsulphate SDS is 0.7 for an aggregation number of 65[24] and 0.5 for an aggregation number of 110[25].

Figure 5 shows results obtained from taking the same approach to treat the $[Cu^{II}(\mathbf{1})(H_2O)_2]Cl_2$ scattering. The fit is again based on the SANS parameters. Whilst the fit is acceptable, it is poorer than we would like. It does however, indicate that the micelles have an obvious prolate character.

Conclusion

Two surfactants differing only by a subtle increase in head group size and coordination chemistry have been examined as functions of surfactant concentration and ionic strength. We have shown that a simple change in surfactant head group structure can result in significant changes in micelle morphology. For both surfactants, the head groups are highly solvated, with approximately 50–60% of the head group region occupied by water. This is not unreasonable given the likelihood of water molecules within the primary and secondary coordination spheres of the complex head groups. The response to added electrolyte (NaCl) and changes in the structure factor, suggests that $[Cu(\mathbf{2})]Cl_2$ has a greater ionic character than $[Cu^{II}(\mathbf{1})(H_2O)_2]Cl_2$, a fact also

reflected in the higher critical micelle concentration for the $[Cu^{II}(\mathbf{2})]Cl_2$ (5 mM) compared to $[Cu^{II}(\mathbf{1})(H_2O)_2]Cl_2$ (0.4 mM).

In the case of $[Cu^{II}(\mathbf{2})]Cl_2$, oblate micelles ($X<1$) are observed, whereas for **1**, the micelles are prolate ($X>1$). The degree of chloride ion dissociation appears to be largely invariant with ionic strength, surfactant concentration and type and indeed close to the assumed value of 0.25.

Acknowledgement

The authors would like to thank the Engineering and Science Research Council (EPSRC) for financial aid (grant GR/R58604/01) and the EPRSC national mass spectrometry for valuable technical support.

[1] a) J. Le Moigne, J. Simon, *J. Phys. Chem.* **1980**, *84*, 170; b) M. Cinquini, F. Montanari, P. Tundo, *J. Chem. Soc. Chem. Commun.* **1975**, 393.

[2] a) R. W. Storrs, F. W. Tropper, H. Y. Li, C. K. Song, J. K. Kuniyoshi, D. A. Sipkins, K. C. P. Li, M. D. Bednarski, M. D. , *J. Am. Chem. Soc.* **1995**, *117*, 7301; b) P. Caravan, M. T. Greenfield, X. D. Li, A. D. Sherry, *Inorg. Chem.* **2001**, *40*, 6580–6587; c) X. D. Li, S. R. Zhang, P. Y. Zhao, Z. Kovacs, A. D. Sherry, *Inorg. Chem.* **2001**, *40*, 6572–6579.

[3] a) H. B. Jervis, M. E. Raimondi, R. Raja, T. Maschmeyer, J. M. Seddon, D. W. Bruce, *Chem. Commun.* **1999**, 2031–2032; b) M. J. Danks, H. B. Jervis, M. Nowotny, W. Zhou, T. Maschmeyer, Bruce, D. W. *Catal. Lett.* **2002**, *82*, 95.

[4] a) P. Ghosh, T. K. Khan, P. K. Bharadwaj, *Chem. Commun.* **1996**, 189–190; b) P. Garcia, J. Marques, E. Pereira, P. Gameiro, R. Salema, B. de Castro, *Chem. Commun.* **2001**, 1298–1299.

[5] C. Moulin, C. Larpent, D. Gazeau, *Anal. Chim. Acta* **1999**, *378*, 47–54.

[6] B. W.-K. Chu, V. W.-W. Yam, *Inorg. Chem* **2001**, *40*, 3324.

[7] R. Wang, Y. Liang, R. H. Schmehl, *Inorg. Chim. Acta* **1994**, *225*, 275–283.

[8] a) K. Manabe, Y. Mori, T. Wakabayashi, S. Nagayama, S. Kobayashi, *J. Am. Chem. Soc.* **2000**, *122*, 7202–7207; b) E. Kimura, H. Hashimoto, T. Koike, *J. Am. Chem. Soc.* **1996**, *118*, 10963–10970.

[9] G. W. Walker, R. J. Geue, A. M. Sargeson, C. A. Behm, *Dalton Trans.* **2003**, 2992–3001.

[10] I. A. Fallis, P. C. Griffiths, P. M. Griffiths, D. E. Hibbs, M. B. Hursthouse, A. L. Winnington, *J. Chem. Soc. Chem. Commun.* **1998**, 665–666.

[11] a) J. Bowers, M. J. Danks, D. W. Bruce, *Langmuir* **2003**, *19*, 292–298; b) E. Caponetti, D. Chillura-Martino, L. Pedone, *J. Appl. Crystallogr.* **2003**, *36*, 753–757; c) M. E. Amato, E. Caponetti, D. C. Martino, L. Pedone, *J Phys. Chem. B* **2003**, *107*, 10048–10056; d) D. Chillura-Martino, E. Caponetti, L. Pedone L, *J. Appl. Crystallogr.* **2003**, *36*, 562–567; e) A. Bumajdad, J. Eastoe, S. Nave, D. C. Steytler, R. K. Heenan, I. Grillo, *Langmuir* **2003**, *19*, 2560–2567; f) P. A. Hassan, G. Fritz, E. W. Kaler, *J. Colloid Interface Sci.* **2003**, *257*, 154–162; g) J. B. Jeong, S. R. Yang, J. D. Kim, *Langmuir* **2002**, *18*, 8749–8755.

[12] a) M. Summers, J. Eastoe, R. M. Richardson, *Langmuir* **2003**, *19*, 6357–6362; b) B. Abecassis, F. Testard, T. Zemb, L. Berthon, C. Madic, *Langmuir* **2003**, *19*, 6638–6644; c) S. F. Santos, D. Zanette, H. Fischer, R. Itri, *J. Colloid Interface Sci.* **2003**, *262*, 400–408; d) Y. Yamashita, H. Kunieda, E. Oshimura, K. Sakamoto, *Langmuir* **2003**, *19*, 4070–4078; e) W. Caetano, L. R. S. Barbosa, R. Itri, M. Tabak, *J. Colloid Interface Sci.* **2003**, *260*, 414–422; f) V. Weber, T. Narayanan, E. Mendes, F. Schosseler, *Langmuir* **2003**, *19*, 992–1000.

[13] a) S. Vass, J. Plestil, P. Laggner, S. Borbely, H. Pospisil, T. Gilanyi, *Phys. B* **2000**, *276*, 406–407; b) M. Ishida, M. Takai, H. Okabayashi, H. Masuda, M. Furusaka, C. J. O'Connor, *Phys. Chem. Chem. Phys.* **2001**, *3*, 3140–3149; c) M. A. Kiselev, P. Lesieur, A. M. Kisselev, D. Lombardo, M. Killany, S. Lesieur S, *J. Alloys Compd.* **2001**, *328*, 71–76; d) L. Z. He, V. M. Garamus, S. S. Funari, M. Malfois, R. Willumeit, B. Niemeyer, *J. Phys. Chem. B* **2002**, *106*, 7596–7604; e) D. J. Iampietro, L. L. Brasher, E. W. Kaler, A. Stradner, O. Glatter, *J. Phys. Chem. B* **1998**, *102*, 3105–3113; f) B. Kunze, J. Kalus, N. Boden, M. S. B. Brandao, *Phys. B* **1997**, *234*, 351–352; g) G. Froba, J. Kalus, *J. Phys. Chem.* **1995**, *99*, 14450–14467; i) J. Eastoe, D. C. Steytler, B. H. Robinson, R. K. Heenan, A. N. Norht, J. C. Dore, *J. Chem. Soc. Faraday Trans* **1994**, *90*, 2497–2504; j) G. Martini, S. Ristori, G. Gebel, A. Chittofrati, M. Visca, *Appl. Magn. Reson.* **1994**, *6*, 29–50; k) G. Gebel, S. Ristori, B. Loppinet, G. Martini, *J. Phys. Chem.* **1993**, *97*, 8664–8668.

[14] L. Arleth, D. Posselt, D. Gazeau, C. Larpent, T. Zemb, K. Mortensen, J. S. Pedersen, *Langmuir* **1997**, *13*, 1887–1896.

[15] K. Wieghardt, W. Schmidt, B. Nuber, J. Weiss, *Chem. Ber.* **1979**, *112*, 2220.

[16] D. D. Perrin, W. F. A. Amarego, *Purification of Laboratory Chemicals* Pergamon Oxford, **1988**.

[17] J. S. Pedersen in *Scattering Methods Applied to Soft Condensed Matter* (Eds.: T. Zemb, P. Lindner), **2002**, Elsevier, pp. 127–144.

[18] a) A. J. Blake, I. A. Fallis, R. O. Gould, S. A. Ross, M. Schröder, *J. Chem. Soc. Chem. Commun.* **1994**, 2467–2469; b) A. J. Blake, I. A. Fallis, S. Parsons, S. A. Ross, M. Schröder, *J. Chem. Soc. Dalton Trans.* **1996**, 31–43.

[19] A. B. P. Lever, *Inorganic Electronic Spectroscopy*, Elsevier **1984**, p. 508.

[20] R. D. Hancock, *Prog. Inorg. Chem.* **1989**, *37*, 187–291.

[21] P. C. Griffiths, A. Y. F. Cheung, G. J. Finney, C. Farley, A. R. Pitt, A. M. Howe, S. M. King, R. K. Heenan, B. L. Bales, *Langmuir* **2002**, *18*, 1065.

[22] E. J. Baerends, *Chem. Phys.* **1973**, *2*, 41.

[23] J. Penfold, E. Staples, L. Thompson, I. Tucker, J. Hines, R. K. Thomas, J. R. Lu, N. Warren, *J. Phys. Chem. B* **1999**, *103*, 5204.

[24] P. C. Griffiths, A. Y. F. Cheung, C. Farley, A. Paul R. K. Heenan, S. M. King, E. Pettersson, P. Stilbs, R. Ranganathan *J. Phys. Chem.* (in press).

[25] P. C. Griffiths, A Paul, R. K. Heenan, J Penfold, R. Ranganathan, Barney L. Bales *Langmuir* (in press).

Received: October 29, 2003
Revised: December 16, 2003 [F5670]